Available online at www.sciencedirect.com
ScienceDirect
Trans. Nonferrous Met. Soc. China 35(2025) 184−193
Transactions of Nonferrous Metals Society of China
www.tnmsc.cn

Influence of Al, Cu and Mn additions on diffusion behaviors in CoCrFeNi high-entropy alloys

Juan CHEN[1,2], Zhen-zhong ZHANG[2], Jin-kun XIAO[2], Li-jun ZHANG[3]

1. Testing Center, Yangzhou University, Yangzhou 225009, China;
2. School of Mechanical Engineering, Yangzhou University, Yangzhou 225009, China;
3. State Key Laboratory of Powder Metallurgy, Central South University, Changsha 410083, China

Received 3 June 2023; accepted 28 December 2023

Abstract: The interdiffusion coefficients in $Al_{0.2}CoCrFeNi$, $CoCrCu_{0.2}FeNi$, and $CoCrFeMn_{0.2}Ni$ high-entropy alloys were efficiently determined by combining diffusion couple experiments and high-throughput determination of interdiffusion coefficients (HitDIC) software at 1273−1373 K. The results show that the addition of Al, Cu, and Mn to CoCrFeNi high-entropy alloys promotes the diffusion of Co, Cr, and Fe atoms. The comparison of tracer diffusion coefficients indicates that there is no sluggish diffusion in tracer diffusion on the thermodynamic temperature scale for the present $Al_{0.2}CoCrFeNi$, $CoCrCu_{0.2}FeNi$, and $CoCrFeMn_{0.2}Ni$ high-entropy alloys. The linear relationship between diffusion entropy and activation energy reveals that the diffusion process of atoms is unaffected by an increase in the number of components as long as the crystal structure remains unchanged.

Key words: Co−Cr−Fe−Ni; high-entropy alloy; diffusion; interdiffusivity; diffusion couple

1 Introduction

High-entropy alloys (HEAs), also known as multi-principal element alloys, usually contain five or more elements in equal or near-equal atomic ratios [1], and have received widespread attention due to their excellent overall properties, such as high strength and ductility [2], high fracture toughness [3], and excellent creep strength [4]. As one of the four “core effects” in HEAs proposed by YEH et al [5], sluggish diffusion has become the research hotspot due to the wide debates on its existence in the literature [6,7]. Moreover, the study of diffusion kinetics in HEAs also helps to assess phase stability and solid-state phase transitions, thereby effectively controlling the kinetic processes during the preparation, processing and use of HEAs and accelerating the process of design and development of new high-performance HEAs [8].

Many researchers have studied the diffusion behavior of HEAs. CHEN et al [9] revealed that the sluggish diffusion only existed for Al, Co, Cr and Ti in fcc Al−Co−Cr−Fe−Ni−Ti HEAs. GAERTNER et al [10] found that Cr, Mn, and Fe in the CoCrFeMnNi HEAs system exhibited significant uphill diffusion. KOTTKE et al [11] reported the sluggish diffusion effect in the equiatomic CoCrFeMnNi HEAs, and the diffusion retardation can be as large as a factor of 30 (Fe) or 10 (Ni) on a homologous temperature scale. TAO et al [12] revealed the diffusion behavior of CuCoCrFeNi HEAs with nickel and copper coating. Cu atoms do not generate lattice diffusion in the CuCoCrFeNi alloy, but they can diffuse at grain boundaries after annealing at high temperature or annealing for long time, while interdiffusion can easily occur between Ni and HEAs. DĄBROWA et al [13] studied the

Corresponding author: Jin-kun XIAO, Tel: +86-15195562127, E-mail: jkxiao@yzu.edu.cn
https://doi.org/10.1016/S1003-6326(24)66673-2

interdiffusion in Co−Cr−Fe−Mn−Ni, Co−Fe−Mn−Ni, Co−Cr−Fe−Ni, Co−Cr−Mn−Ni, and Al−Co−Cr−Fe−Ni, and there is no signs of diffusion retardation in HEAs when the absolute temperature scale is considered. And sluggish diffusion occurs only for alloys with prominent manganese content in HEAs and binary systems. The above researches [9−13] indicate that HEAs with different alloying elements exhibit different diffusion behaviors. However, the effect of their additions on the interdiffusion coefficient in fcc HEAs has rarely been discussed. Therefore, it is necessary to study the influence of different alloying elements on the diffusion behavior of HEAs. What' more, understanding the effect of the additional elements on the diffusion behaviors in alloys helps to design the high-performance alloys to meet the usage requirements [14].

Al, Cu, and Mn are common additional elements in fcc-based HEAs [6,15,16]. The influence of Al, Cu and Mn additions on diffusion behaviors in CoCrFeNi high-entropy alloys is chosen as the target in the present work. The major objectives are: (1) to determine the interdiffusion coefficients of $Al_{0.2}CoCrFeNi$, $CoCrCu_{0.2}FeNi$ and $CoCrFeMn_{0.2}Ni$ HEAs by combining the diffusion couple experiments and high-throughput determination of interdiffusion coefficients (HitDIC) software; (2) to discuss the effect of the addition of Al, Cu and Mn on the interdiffusion coefficients in fcc CoCrFeNi HEAs; (3) to analyze the influence of diffusion entropy on the tracer diffusion coefficients and the premise of sluggish diffusion in CoCrFeNi-based HEAs.

2 Experimental

Metal rods of pure Al (purity: 99.99%), Co (purity: 99.95%), Cr (purity: 99.95%), Cu (purity: 99.99%), Fe (purity: 99.9%), Mn (purity: 99.9%), and Ni (purity: 99.98%) were added to prepare $Al_{0.2}CoCrFeNi$, $CoCrCu_{0.2}FeNi$, $CoCrFeMn_{0.2}Ni$ and CoCrFeNi HEAs in a vacuum arc melting furnace under a purified Ar atmosphere. The HEA ingots were melted and re-melted at least five times to ensure homogenous composition. The as-cast buttons were subsequently homogenized in a high-temperature tube furnace (GSL1700X) at 1373 K for 7 d. After being quenched in cold water, the homogenized alloys were subjected to X-ray diffraction (XRD, D8 Advance) technique for phase identification.

Subsequently, the homogenized buttons were cut into small pieces with size of 5 mm × 5 mm × 1.8 mm. All samples were ground to remove any contaminant, and one face with a dimension of 5 mm × 5 mm of the samples was polished. The polished faces of homogenized samples were fitted together, and assembled by Mo fixture to prepare the diffusion couples, as listed in Table 1.

Table 1 Actual compositions for end-members of different diffusion couples together with their diffusion treatment in this work

Couple No.	Actual composition/at.%	Temperature/ K	Diffusion time/h
A1	24.7Co−26.3Cr−24.8Fe−24.2Ni	1273	71
B1		1323	65
C1		1373	48
A2	24.7Co−26.3Cr−24.8Fe−4.8Cu−23.5Fe−23.1Ni	1273	71
B2		1323	65
C2		1373	48
A3	24.7Co−26.3Cr−24.8Fe−23.6Fe−4.1Mn−23.3Ni	1273	71
B3		1323	65
C3		1373	48

Diffusion couples were sealed in a quartz tube with a vacuum environment, and then they were annealed at 1273, 1323, and 1373 K for 71, 65, and 48 h, respectively, followed by water quenching. After that, the cross section of each diffusion couple was ground and polished by standard metallographic techniques, and the microstructure was then characterized by scanning electron microscopy (SEM, Gemini 300). The composition profiles on the straight line along the vertical diffusion interface were analyzed with the electron probe microanalyzer (EPMA, JXA-8230).

3 Results and discussion

3.1 Concentration profiles

The actual compositions of $Al_{0.2}CoCrFeNi$, $CoCrCu_{0.2}FeNi$, $CoCrFeMn_{0.2}Ni$, and CoCrFeNi HEAs are determined by EPMA as 4.5Al−23.6Co−25.1Cr−23.6Fe−23.2Ni, 23.4Co−25.2Cr−4.8Cu−23.5Fe−23.1Ni, 23.6Co−25.4Cr−23.6Fe−4.1Mn−23.3Ni, and 24.7Co−26.3Cr−24.8Fe−24.2Ni (at.%),

respectively. According to our previous work and literature reports [6,7,17−19], CoCrFeNi, $Al_{0.2}$CoCrFeNi, $CoCrCu_{0.2}$FeNi, and $CoCrFeMn_{0.2}$Ni alloys prepared in this work locate in fcc single-phase region. To further identify the phases in the HEAs prepared in this work, XRD patterns of four HEAs were measured and shown in Fig. 1. It can be observed in Fig. 1 that CoCrFeNi, $Al_{0.2}$CoCrFeNi, $CoCrCu_{0.2}$FeNi, and $CoCrFeMn_{0.2}$Ni alloys exhibit a typical fcc single phase.

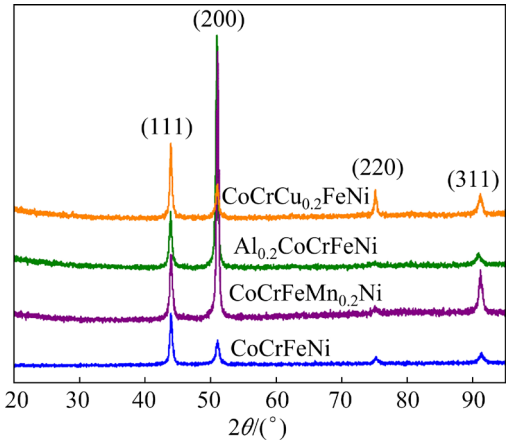

Fig. 1 XRD patterns of as-homogenized CoCrFeNi, $CoCrFeMn_{0.2}$Ni, $Al_{0.2}$CoCrFeNi, and $CoCrCu_{0.2}$FeNi alloys

A representative backscattered electron image (BEI) of B2 (CoCrFeNi/$Al_{0.2}$CoCrFeNi) diffusion couple, which was annealed at 1323 K for 65 h, is depicted in Fig. 2. As can be seen from Fig. 2, CoCrFeNi and $Al_{0.2}$CoCrFeNi alloys on both sides of the B2 diffusion couple possess a homogeneous structure, and no second phase precipitation is observed. Thus, the BEI of CoCrFeNi and $Al_{0.2}$CoCrFeNi alloys also indicates a single-phase microstructure.

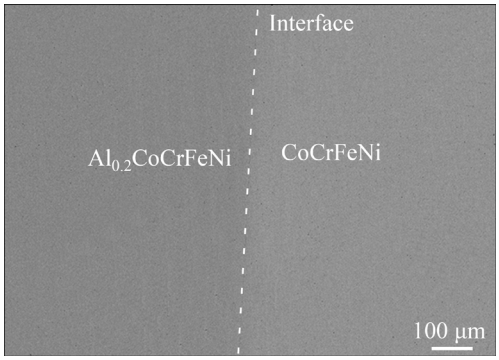

Fig. 2 Representative backscattered electron image of B2 diffusion couple annealed at 1323 K for 65 h

Figure 3 presents experimental composition profiles of diffusion couples for AlCoCrFeNi, CoCrCuFeNi, and CoCrFeMnNi systems at 1273−1373 K. As displayed in Fig. 3, the composition profiles for all elements are S-shaped, which indicates that interdiffusion between the alloys occurs. Besides, under the same diffusion conditions, Al, Cu and Mn have greater diffusion depths than Co, Cr and Fe in the same alloy systems, inferring diffusion rates of Al, Cu and Mn are generally larger than those of Co, Cr and Fe. Based on the experimental composition profiles, the mobility parameters together with the interdiffusion coefficients in AlCoCrFeNi, CoCrCuFeNi and CoCrFeMnNi systems were evaluated by using the HitDIC software, which has been widely used for the evaluation of interdiffusion coefficients of binary, ternary and even multicomponent/multi-principal element alloys [20,21]. Meanwhile, Fig. 3 also shows the simulated composition profiles generated by the HitDIC software. As seen in Fig. 3, all the experimental data can be well reproduced by the simulated results.

3.2 Interdiffusivity matrices

Figure 4 shows the evaluated main interdiffusion coefficients for AlCoCrFeNi, CoCrCuFeNi, and CoCrFeMnNi systems at 1273−1373 K. It can be clearly seen from Fig. 4 that the interdiffusivities increase with the increase of temperature. In AlCoCrFeNi system, Al has the largest inter-diffusion coefficient, followed by Fe, Co, and Cr. In CoCrCuFeNi system, the order of the interdiffusion coefficients is Cu > Fe > Cr > Co. In CoCrFeMnNi systems, Mn possesses the largest interdiffusivities, followed by Cr, Fe, and Co. The facts indicate that the additions of Al, Cu and Mn in CoCrFeNi have different effects on the interdiffusion coefficients of Co, Cr and Fe.

The presently evaluated interdiffusivities are compared with the reported results in the literature [6,18,19,22], as displayed in Fig. 5. As can be seen in Fig. 5, the differences between the presently evaluated interdiffusion coefficients in AlCoCrFeNi, CoCrCuFeNi, and CoCrFeMnNi systems and those reported in Refs. [6,18,19,22] are with half an order of magnitude, indicating that the interdiffusion coefficients evaluated in this work are reliable.

In order to analyze the effect of the addition of Al, Cu and Mn on the interdiffusion coefficients of

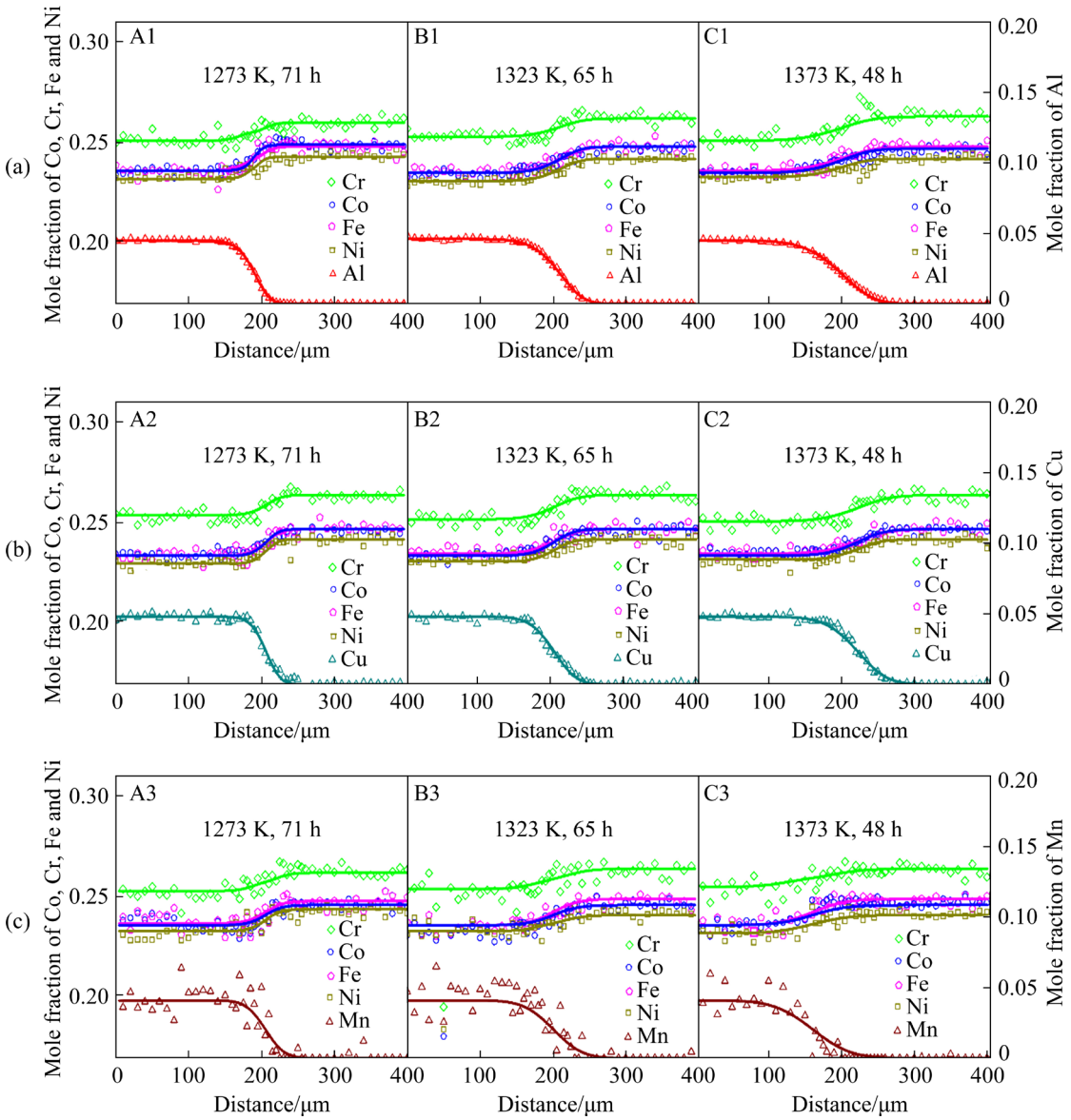

Fig. 3 Experimental composition profiles (symbols) and simulated values (solid lines) of A1, B1, and C1 diffusion couples in AlCoCrFeNi (a), A2, B2, and C2 diffusion couples in CoCrCuFeNi (b), and A3, B3, and C3 diffusion couples in CoCrFeMnNi (c) systems under different diffusion conditions

Co, Cr and Fe in the CoCrFeNi HEAs, respectively, the interdiffusivities in CoCrFeNi, $Al_{0.2}$CoCrFeNi, CoCr$Cu_{0.2}$FeNi and CoCrFe$Mn_{0.2}$Ni alloys at 1273−1373 K are compared in Fig. 6. As shown in Fig. 6, the interdiffusion coefficients of Co, Cr and Fe in $Al_{0.2}$CoCrFeNi, CoCr$Cu_{0.2}$FeNi and CoCrFe$Mn_{0.2}$Ni alloys are greater than their interdiffusivities in the CoCrFeNi alloy. This fact indicates that the addition of Al, Cu, and Mn enhances the interdiffusion coefficients of Co, Cr, and Fe in CoCrFeNi alloy. The similar phenomenon has been already reported in the literature [6,18,23]. The reason might be that the addition of Al, Cu, and Mn in the CoCrFeNi HEAs lowers the melting point of the alloy. Under this situation, at a given temperature, the alloy owns a higher equilibrium concentration of vacancies, accelerating the substitutional diffusion [23]. Moreover, the increase in the interdiffusion coefficients of Cr and Fe in the $Al_{0.2}$CoCrFeNi alloy is greater than that of Co. The interdiffusion coefficients of Fe/Cr on the $Al_{0.2}$CoCrFeNi alloy side in the $Al_{0.2}$CoCrFeNi/CoCrFeNi diffusion couple are about twice as high as those on the CoCrFeNi alloy side. The increase in the interdiffusivities of Co, Cr, and Fe in CoCr$Cu_{0.2}$FeNi and CoCrFe$Mn_{0.2}$Ni alloys shows

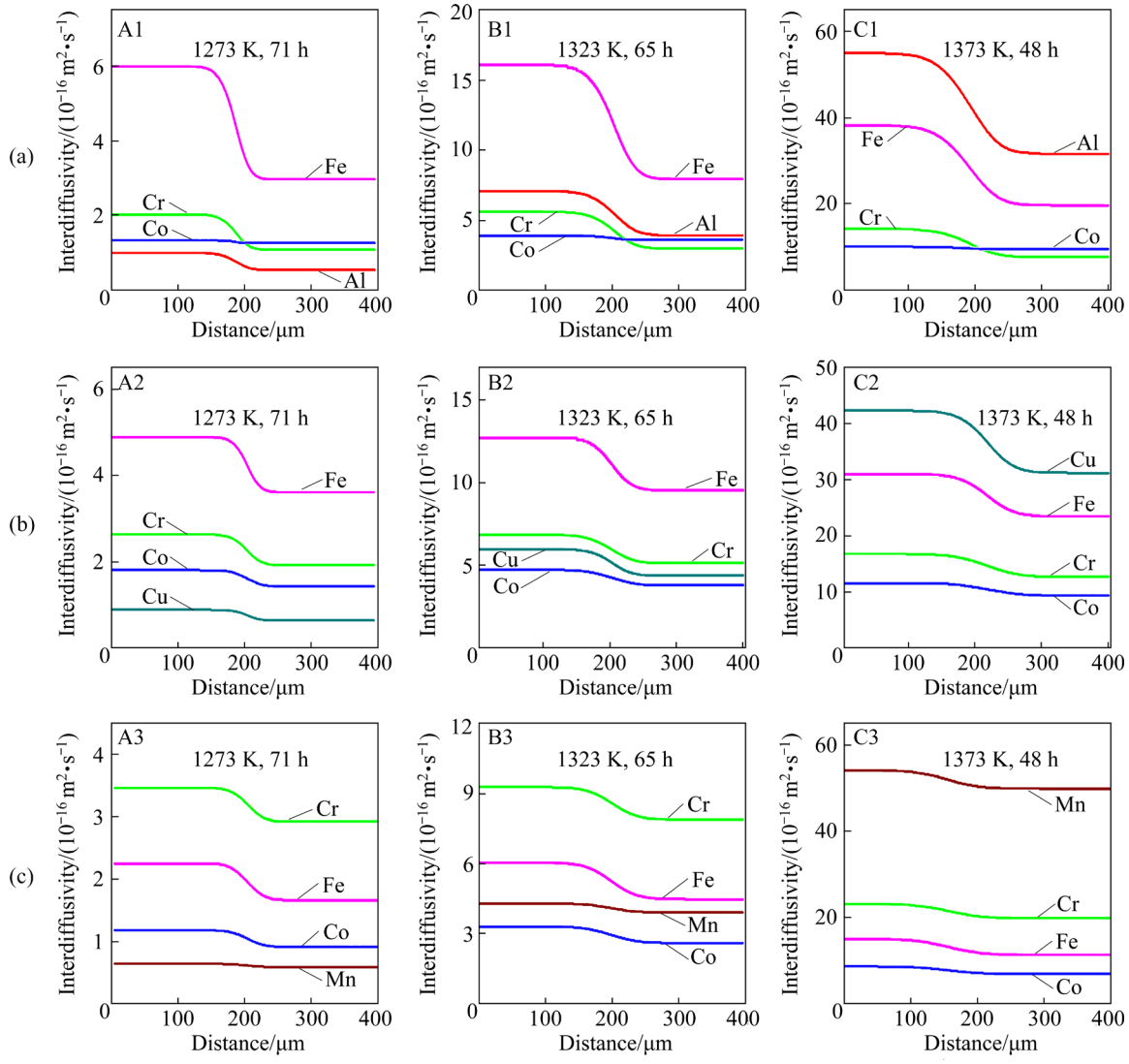

Fig. 4 Main interdiffusivities calculated for A1, B1, and C1 diffusion couples in AlCoCrFeNi (a), A2, B2, and C2 diffusion couples in CoCrCuFeNi (b), and A3, B3, and C3 diffusion couples in CoCrFeMnNi (c) systems at 1273−1373 K

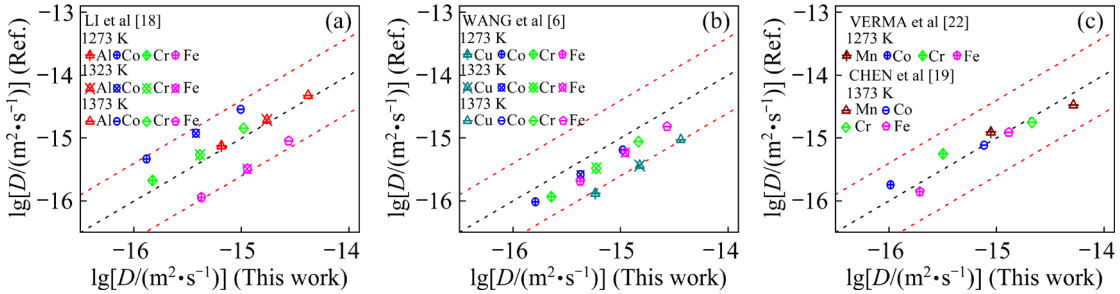

Fig. 5 Comparison between interdiffusivities in AlCoCrFeNi (a), CoCrCuFeNi (b), and CoCrFeMnNi (c) systems from reference [6,18,19,22] and present work

little difference. This suggests that Al has a greater effect on the interdiffusivities of Cr and Fe than on Co. In contrast, the effects of Cu and Mn on the interdiffusivities of Co, Cr, and Fe do not differ significantly.

$\tilde{D}_{ij}^{N}$ is the cross interdiffusion coefficient, which refers to the effect of j on the interdiffusion coefficient of i in the alloy system with solvent N. Figure 7 illustrates the calculated cross inter-diffusivities for A1, B1, and C1 diffusion couples in

AlCoCrFeNi, A2, B2, and C2 diffusion couples in CoCrCuFeNi, and A3, B3, and C3 diffusion couples in CoCrFeMnNi systems at 1273−1373 K. It can be observed from Fig. 7(a) that $\left|\tilde{D}^{\mathrm{Ni}}_{\mathrm{CrAl}}\right|$, $\left|\tilde{D}^{\mathrm{Ni}}_{\mathrm{CoAl}}\right|$ and $\left|\tilde{D}^{\mathrm{Ni}}_{\mathrm{FeAl}}\right|$ are larger than the other cross interdiffusivities, Fig. 7(b) shows that $\left|\tilde{D}^{\mathrm{Ni}}_{\mathrm{CrCu}}\right|$, $\left|\tilde{D}^{\mathrm{Ni}}_{\mathrm{CoCu}}\right|$ and $\left|\tilde{D}^{\mathrm{Ni}}_{\mathrm{FeCu}}\right|$ are the maximum, and Fig. 7(c) indicates that $\left|\tilde{D}^{\mathrm{Ni}}_{\mathrm{CrMn}}\right|$, $\left|\tilde{D}^{\mathrm{Ni}}_{\mathrm{CoMn}}\right|$ and $\left|\tilde{D}^{\mathrm{Ni}}_{\mathrm{FeMn}}\right|$ are the largest. This suggests that the effect of the added elements of Al, Cu, and Mn on the interdiffusion coefficients of atoms in CoCrFeNi alloy is greater than that of Co, Cr, and Fe atoms on the interdiffusivities of other atoms. What's more, $\left|\tilde{D}^{\mathrm{Ni}}_{\mathrm{CrAl}}\right|$, $\left|\tilde{D}^{\mathrm{Ni}}_{\mathrm{CoAl}}\right|$ and $\left|\tilde{D}^{\mathrm{Ni}}_{\mathrm{FeAl}}\right|$ on the $Al_{0.2}$CoCrFeNi alloy side in the A1, B1, and C1 diffusion couples are about 1.7 times as high as those on the CoCrFeNi

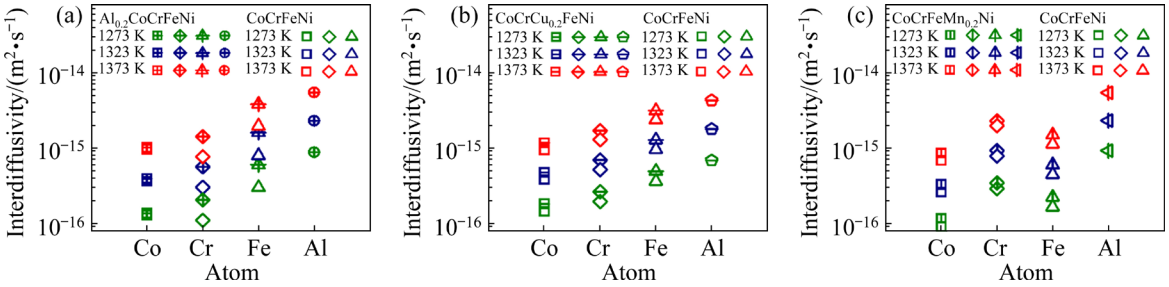

Fig. 6 Comparisons between interdiffusivities in $Al_{0.2}$CoCrFeNi (a), CoCrCu$_{0.2}$FeNi (b), CoCrFeMn$_{0.2}$Ni (c) alloys and those in CoCrFeNi alloys at 1273−1373 K

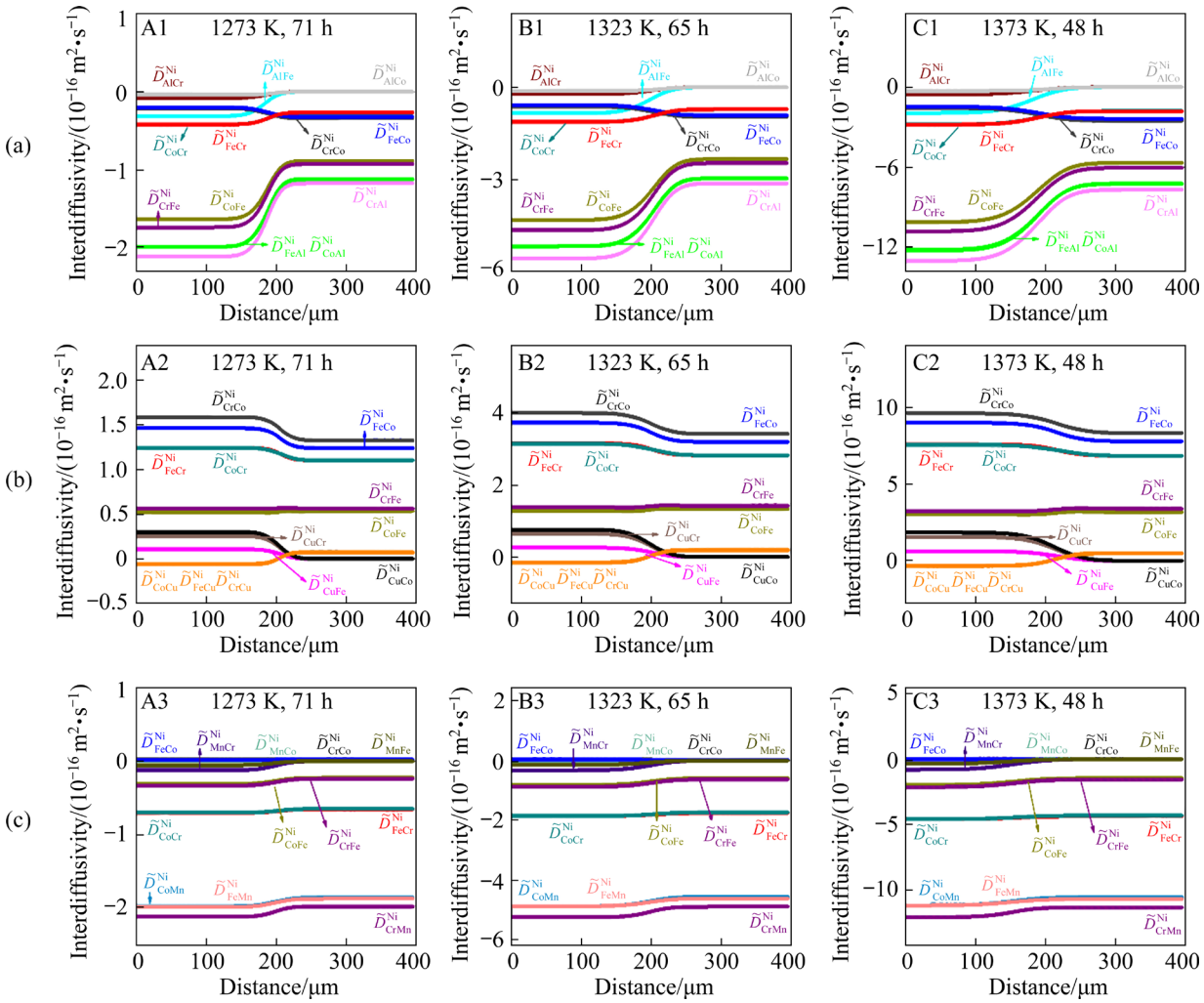

Fig. 7 Cross interdiffusivities calculated for A1, B1, and C1 diffusion couples in AlCoCrFeNi (a), A2, B2, and C2 diffusion couples in CoCrCuFeNi (b), and A3, B3, and C3 diffusion couples in CoCrFeMnNi (c) systems at 1273−1373 K

alloy side. In contrast, all the cross interdiffusion coefficients in the A2, B2, C2, A3, B3, and C3 diffusion couples on the CoCrCuFeNi/CoCrFeMnNi and CoCrFeNi alloy sides are not significantly different. Therefore, the addition of Al has a greater effect on the interdiffusion coefficients of atoms in CoCrFeNi alloys than the addition of Cu and Mn.

3.3 Effect of diffusion entropies on diffusion coefficients

The tracer diffusion coefficient (D_i^*) can be calculated from the mobility parameter (M_i) by Einstein formula (D_i^* =RTM_i). The tracer diffusivities evaluated in the present work as a function of reciprocal of temperature are given in Fig. 8, compared with the reported data in different fcc alloy systems: pure Ni [24], pure Co [25], pure Cu [26], pure Fe [27], Al in Ni [28], Co in Ni [29], Cr in Ni [30], Fe in Ni [31], Mn in Ni [32], $FeCr_{15}Ni_{45}$ [33], $Co_{25}Cr_{25}Fe_{25}Ni_{25}$ [34], $Co_{20}Cr_{20}Fe_{20}Mn_{20}Ni_{20}$ [34]. As can be seen, the tracer diffusion coefficients of Al, Cu and Mn in the HEAs determined in this work are smaller than the self-diffusion coefficients of the pure metals or impurity diffusion coefficients of alloys. The tracer diffusion coefficients of Cr in the HEAs are smaller than those of Cr in Ni and close to those of Cr in the $FeCr_{15}Ni_{45}$ alloy. The tracer diffusion coefficients of Co, Fe and Ni in HEAs are even higher than some tracer diffusion coefficients in pure metals or conventional alloys. It can be inferred from Fig. 8 that the tracer diffusion coefficients in $Al_{0.2}$CoCrFeNi, $CoCrCu_{0.2}$FeNi and $CoCrFeMn_{0.2}$Ni HEAs might not have sluggish phenomenon, which is consistent with the findings in literature [6,18,23].

The temperature-dependent tracer diffusion coefficient follows the Arrhenius formula ($D^*=D_0\exp[-Q/(RT)]$. Here, Q is the activation energy, D_0 is the pre-exponential factor, T is the thermodynamic temperature and R is the molar gas constant. Activation energy and pre-exponential factors for tracer diffusivities of the components in $Al_{0.2}$CoCrFeNi, $CoCrCu_{0.2}$FeNi and $CoCrFeMn_{0.2}$Ni HEAs are plotted in Fig. 9. In general, larger diffusion coefficients correspond to lower diffusion

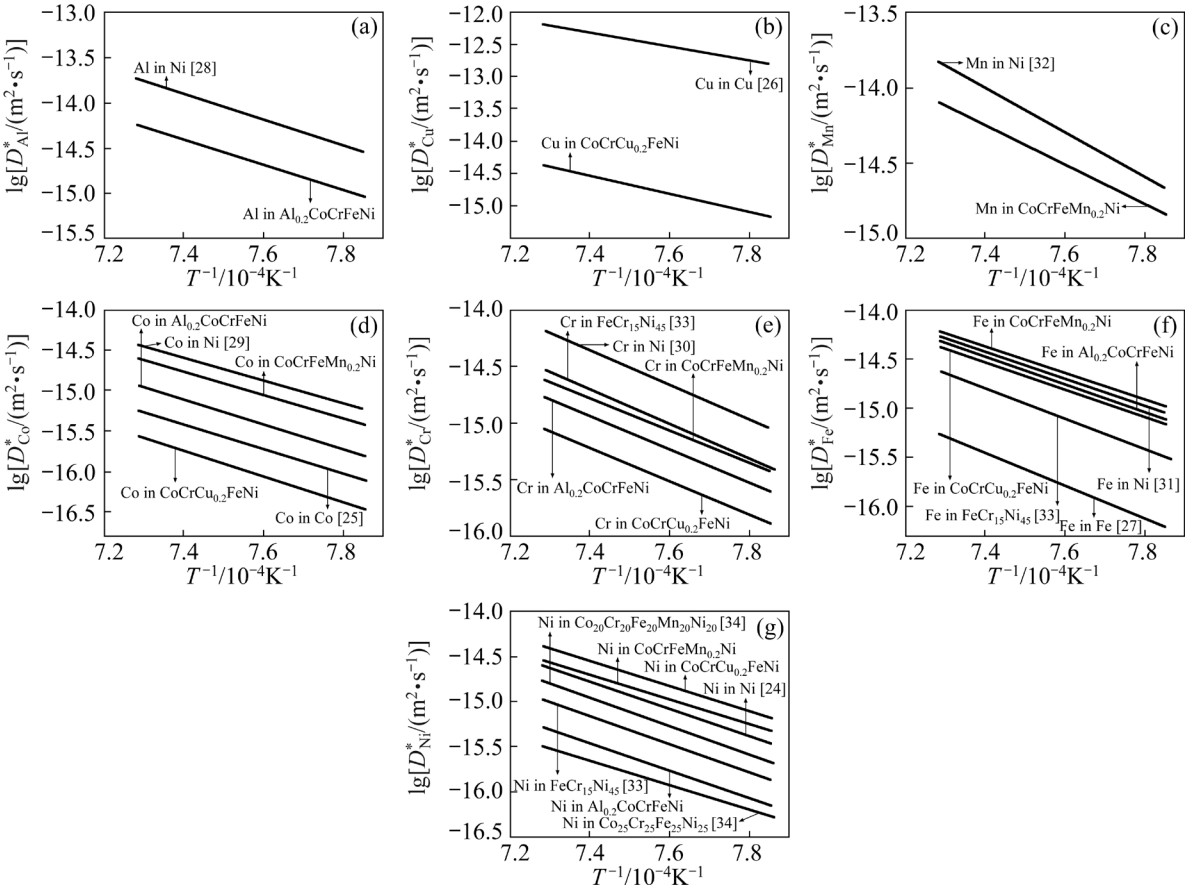

Fig. 8 Comparisons of tracer diffusivities D_{Al}^* (a), D_{Cu}^* (b), D_{Mn}^* (c), D_{Co}^* (d), D_{Cr}^* (e), D_{Fe}^* (f) and D_{Ni}^* (g) calculated in present work with reported data in different fcc alloy systems

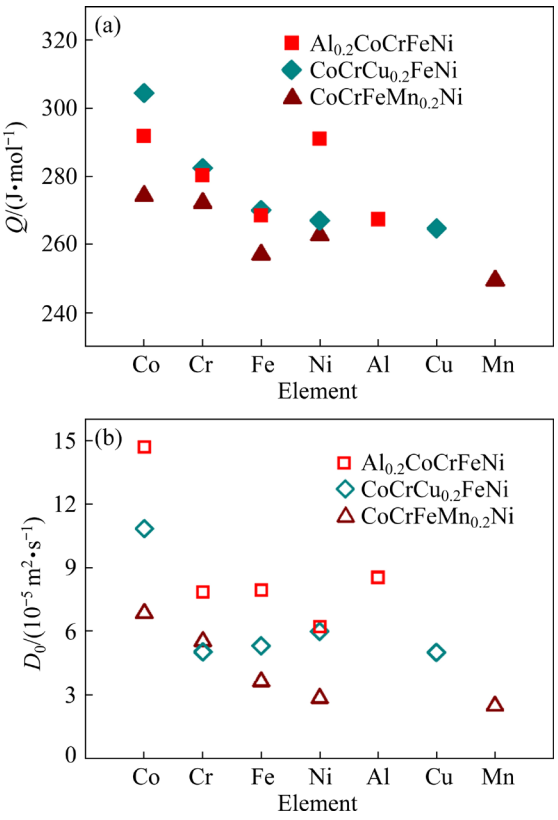

Fig. 9 Activation energy (a) and pre-exponential factors (b) for tracer diffusivities of components in $Al_{0.2}CoCrFeNi$, $CoCrCu_{0.2}FeNi$ and $CoCrFeMn_{0.2}Ni$ HEAs

activation energies. As shown in Fig. 9(a), Mn, Cu, and Al have lower diffusion activation energy than Co, Cr, Fe, and Ni in the same system. As shown in Fig. 9(b), the relationship between the magnitude of the pre-exponential factor and the diffusion coefficient is not obvious. D_0 is often derived from the formula $D_0=gfa^2\nu_0\exp(\Delta S/R)$ [35]. Here, f is correlation factor, g is geometric factor, a is lattice parameter, ν_0 is attempt frequency, and ΔS is diffusion entropy. For FCC lattice, g=1, and f=0.787. ν_0 can be taken as the Debye frequency (10^{13} s^{-1}). The lattice parameters for $Al_{0.2}CoCrFeNi$, $CoCrCu_{0.2}FeNi$ and $CoCrFeMn_{0.2}Ni$ HEAs obtained from the XRD patterns in Fig. 1 are 0.358, 0.359, and 0.358 nm.

Figure 10 shows diffusion entropy, $\Delta S/R$, as a function of the corresponding diffusion activation energy of the components in pure metals, binary, ternary, and HEAs [23,25,33,36−39]. Figure 10 indicates that the diffusion entropies are linearly related to activation energies for a wide range of fcc alloys, which has been observed in the literature [23]. The linear relationship between diffusion entropy and activation energy in fcc-phase HEAs and low-component alloys hints that the addition of components in HEAs might not alter the atomic diffusion process, provided the crystal structure remains unchanged.

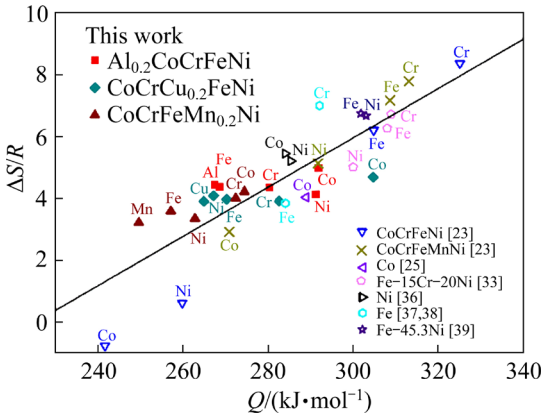

Fig. 10 Diffusion entropy ($\Delta S/R$) as function of corresponding diffusion activation energy of components in pure metals, and HEAs [23,25,33, 36−39]

4 Conclusions

(1) Nine groups of fcc solid/solid diffusion couples for $Al_{0.2}CoCrFeNi$, $CoCrCu_{0.2}FeNi$, and $CoCrFeMn_{0.2}Ni$ high-entropy alloy systems were prepared. After diffusion annealing at 1273, 1323, and 1373 K, the composition profiles were measured by electron probe, and the composition-dependent interdiffusivities were determined with the aid of HitDIC software.

(2) The interdiffusivities of Co, Cr, and Fe in the $Al_{0.2}CoCrFeNi$, $CoCrCu_{0.2}FeNi$, and $CoCrFeMn_{0.2}Ni$ HEAs are greater than those in the CoCrFeNi HEAs. Al has a greater effect on the interdiffusion coefficients of atoms in CoCrFeNi alloys than Cu and Mn. Comparison between the tracer diffusivities determined in this work and the data available in the literature reveals that there is no sluggish diffusion effect in the tracer diffusivities.

(3) Al, Cu, and Mn atoms that have higher diffusion coefficients have lower diffusion activation energies, while their pre-exponential factors are not significantly related to the diffusion coefficients. In addition, the diffusion entropies of fcc-phase HEAs and low-component alloys exhibit a linear relationship with the diffusion activation energy.

CRediT authorship contribution statement

Juan CHEN: Conceptualization, Investigation, Funding acquisition, Writing − Original draft, Writing − Review & editing; **Zhen-zhong ZHANG:** Investigation, Methodology, Visualization, Writing − Original draft; **Jin-kun XIAO:** Investigation, Methodology, Validation; **Li-jun ZHANG:** Resources, Validation, Writing − Review & editing.

Declaration of competing interest

The authors declare that they have no known competing financial interests or personal relationships that could have appeared to influence the work reported in this paper.

Acknowledgments

This work was supported by the National Natural Science Foundation of China (No. 52374372), the Natural Science Foundation of the Jiangsu Higher Education Institutions of China (No. 23KJB430042), the Jiangsu Province Large Scientific Instruments Open Sharing Autonomous Research Filing Project, China (No. TC2023A037), the Yangzhou City−Yangzhou University Cooperation Foundation, China (No. YZ2022183), High-end Talent Support Program of Yangzhou University, China, Qinglan Project of Yangzhou University, China, and Lvyangjinfeng Talent program of Yangzhou, China.

References

[1] MURTY B S, YEH J W, RANGANATHAN S, BHATTACHARJEE P P. High entropy alloys [M]. 2nd ed. Amsterdam: Elsevier, 2019.

[2] TONG Y G, TIAN N, CHEN H, ZHANG X C, HU Y L, JI X X, ZHANG M J, ZHAO C J. Real-time atomic deformation behavior of nano CoCrCuFeNi high-entropy alloy [J]. Transactions of Nonferrous Metals Society of China, 2023, 33: 1156−1163.

[3] MA Z H, HOU B, QIN D Y, LI Y L. Effect of strain rate on mechanical properties of HCP/FCC dual-phase CoCrFeNi-$Nb_{0.5}$ high-entropy alloy [J]. Transactions of Nonferrous Metals Society of China, 2023, 33: 1144−1155.

[4] LI R D, NIU P D, YUAN T C, LI Z M. Displacive transformation as pathway to prevent micro-cracks induced by thermal stress in additively manufactured strong and ductile high-entropy alloys [J]. Transactions of Nonferrous Metals Society of China, 2021, 31: 1059−1073.

[5] YEH J W, CHEN S K, LIN S J, GAN J Y, CHIN T S, SHUN T T, TSAU C H, CHANG S Y. Nanostructured high-entropy alloys with multiple principal elements: Novel alloy design concepts and outcomes [J]. Advanced Engineering Materials, 2004, 6: 299−303.

[6] WANG R, CHEN W M, ZHONG J, ZHANG L J. Experimental and numerical studies on the sluggish diffusion in face centered cubic Co−Cr−Cu−Fe−Ni high-entropy alloys [J]. Journal of Materials Science & Technology, 2018, 34: 1791−1798.

[7] CHEN J, XIAO J K, ZHANG L J. Interdiffusion behaviors between NiCrFe alloy and low-/medium-/high-entropy alloys [J]. Journal of Alloys and Compounds, 2021, 896: 162711.

[8] XIAO B, LUAN J H, ZHAO S J, ZHANG L J, CHEN S Y, ZHAO Y L, XU L Y, LIU C T, KAI J J, YANG T. Achieving thermally ultra-stable nanoparticles in chemically complex NiCoFeCrAlTi-type alloys via the controllable sluggish lattice diffusion [J]. Nature Communications, 2022, 13: 4870.

[9] CHEN S Y, LI Q, ZHONG J, XING F Z, ZHANG L J. On diffusion behaviors in face centered cubic phase of Al−Co−Cr−Fe−Ni−Ti high-entropy superalloys [J]. Journal of Alloys and Compounds, 2019, 791: 255−264.

[10] GAERTNER D, ABRAHAMS K, KOTTKE J, ESIN V A, STEINBACH I, WILDE G, DIVINSKI S V. Concentration-dependent atomic mobilities in FCC CoCrFeMnNi high-entropy alloys [J]. Acta Materialia, 2019, 166: 357−370.

[11] KOTTKE J, LAURENT-BROCQ M, FAREED A, GAERTNER D, PERRIERE L, ROGAL Ł, DIVINSKI S V, WILDE G. Tracer diffusion in the Ni−CoCrFeMn system: Transition from a dilute solid solution to a high entropy alloy [J]. Scripta Materialia, 2019, 159: 94−98.

[12] TAO W J, ZHANG W Q, FU H M. Diffusion behavior of Cu and Ni atoms in CuCoCrFeNi high entropy alloy [J]. Transactions of Materials and Heat Treatment, 2017, 38: 34−39.

[13] DABROWA J, ZAJUSZ M, KUCZA W, CIESLAK G, BERENT K, CZEPPE T, KULIK T, DANIELEWSKI M. Demystifying the sluggish diffusion effect in high entropy alloys [J]. Journal of Alloys and Compounds, 2019, 783: 193−207.

[14] CHEN J, ZHANG L J, LU X G. Screening of possible Re-substitutional elements in single-crystal Ni-based superalloys: A viewpoint from interdiffusion coefficients in Ni−Al−X ternaries [J]. Metallurgical and Materials Transactions A—Physical Metallurgy and Materials Science, 2018, 49: 2999−3010.

[15] ZHONG J, CHEN L, ZHANG L J. Automation of diffusion database development in multicomponent alloys from large number of experimental composition profiles [J]. npj Computational Materials, 2021, 7: 320−332.

[16] ZHONG J, LI Q, DENG C M, ZHANG L J. Automated development of an accurate diffusion database in fcc AlCoCrFeNi high-entropy alloys from a big dataset of composition profiles [J]. Materials, 2022, 15: 3240.

[17] CHEN J, XU G M, XIAO J K, ZHANG L J. Experimental investigations on the quinary interdiffusivities in diffusion couples of NiAlCoCr alloy/CoCrFeNi high-entropy alloys [J]. CALPHAD, 2022, 76: 102388.

[18] LI Q, CHEN W M, ZHONG J, ZHAGN L J, CHEN Q, LIU Z K. On sluggish diffusion in fcc Al−Co−Cr−Fe−Ni high-entropy alloys: An experimental and numerical study [J]. Metals, 2018, 8: 16.

[19] CHEN W M, ZHANG L J. High-throughput determination of interdiffusion coefficients for Co−Cr−Fe−Mn−Ni high-entropy alloys [J]. Journal of Phase Equilibria and Diffusion, 2017, 38: 457−465.

[20] LIN H Q, LING J F, CHEN W M, WANG Y, WU X K, ZHANG L J. High-throughput determination of mechanical and diffusion properties of Ti−Ta−Fe alloys [J]. Transactions of Nonferrous Metals Society of China, 2022, 32: 3963−3972.

[21] ZHONG J, CHEN L, ZHANG L J. High-throughput determination of high-quality interdiffusion coefficients in metallic solids: A review [J]. Journal of Materials Science, 2020, 55: 10303−10338.
[22] VERMA V, TRIPATHI A, KULKARNI K N. On interdiffusion in FeNiCoCrMn high entropy alloy [J]. Journal of Phase Equilibria and Diffusion, 2017, 38: 445−456.
[23] VAIDYA M, PRADEEP K G, MURTY B S, WILDE G, DIVINSKI S V. Bulk tracer diffusion in CoCrFeNi and CoCrFeMnNi high entropy alloys [J]. Acta Materialia, 2018, 146: 211−224.
[24] BAKKER H. A curvature in the In D versus 1/T plot for self-diffusion in nickel at temperatures from 980 to 1400 °C [J]. Physica Status Solidi B−Basic Research, 1968, 28: 569−576.
[25] BUSSMANN W, HERZIG C, REMPP W, MAIER K, MEHRER H. Isotope effect and self-diffusion in face-centered cubic cobalt [J]. Physica Status Solidi A—Applied Research, 1979, 56: 87−97.
[26] ANUSAVICE K J, DEHOFF R T. Diffusion of the tracers Cu^{66}, Ni^{66}, and Zn^{65} in copper-rich solid solutions in the system Cu−Ni−Zn [J]. Metallurgical Transactions, 1972, 3: 1279−1298.
[27] IVANTSOV I G, BLINKIN A M. Self-diffusion in strongly diluted binary solution. III. Effect of tin, antimony, lead, and bismuth impurities on the self-diffusion of iron in the γ-phase [J]. Physics of Metals and Metallography, 1966, 22: 876−883.
[28] LEE C G, YOUN K T, CHO H H, LEE Y I, YOO D S, SHIMOZAKI T. Measurement of the impurity diffusion of Al in Ni by laser induced breakdown spectrometry (LIBS) [J]. Defect Diffusion Forum, 2001, 194/195/196/197/198/199: 109−114.
[29] HIRANO K I, AGARWALA R P, AVERBACH B L, COHEN M. Diffusion in cobalt-nickel alloys [J]. Journal of Applied Physics, 1962, 33: 3049−3054.
[30] RŮŽIČKOVÁ J, MILLION B. Self-diffusion of the components in the F.C.C. phase of binary solid solutions of the Fe−Ni−Cr system [J]. Materials Science and Engineering, 1981, 50: 59.
[31] HEUER C F. Diffusion of iron and cobalt in nickel single crystals [D]. Rolla: University of Missouri- Rolla, 1969.
[32] SWALIN R A, MARTIN A. Solute diffusion in nickel-base substitutional solid solutions [J]. JOM, 1956, 8: 567−571.
[33] ROTHMAN S, NOWICKI L, MURCH G. Self-diffusion in austenitic Fe−Cr−Ni alloys [J]. Journal of Physics F: Metal Physics, 1980, 10: 383.
[34] VAIDYA M, TRUBEL S, MURTY B S, WILDE G, DIVINSKI S V. Ni tracer diffusion in CoCrFeNi and CoCrFeMnNi high entropy alloys [J]. Journal of Alloys and Compounds, 2016, 688: 994−1001.
[35] DIENES G J. Frequency factor and activation energy for the volume diffusion of metals [J]. Journal of Applied Physics, 1950, 21: 1189−1192.
[36] NEUMANN G, TUIJN C. Self-diffusion and impurity diffusion in pure metals: Handbook of experimental data [M]. Amsterdam: Elsevier, 2011.
[37] BOWEN A W, LEAK G M. Solute diffusion in alpha- and gamma-iron [J]. Metallurgical Transactions, 1970, 1: 1695−1700.
[38] HEUMANN T, IMM R. Self-diffusion and isotope effect in γ-iron [J]. Journal of Physics and Chemistry of Solids, 1968, 29: 1613−1621.
[39] MILLION B, RŮŽIČKOVÁ J, VELÍŠEK J, VŘEŠTÁL J. Diffusion processes in the FeNi system [J]. Materials Science and Engineering, 1981, 50: 43−52.

Al、Cu 和 Mn 添加对 CoCrFeNi 高熵合金扩散行为的影响

陈 娟[1,2]，张振忠[2]，肖金坤[2]，张利军[3]

1. 扬州大学 测试中心，扬州 225009；
2. 扬州大学 机械工程学院，扬州 225009；
3. 中南大学 粉末冶金国家重点实验室，长沙 410083

摘 要：通过扩散偶实验和高通量测定扩散系数(HitDIC)软件相结合，测定了 $Al_{0.2}$CoCrFeNi、CoCr$Cu_{0.2}$FeNi 和 CoCrFe$Mn_{0.2}$Ni 高熵合金在 1273~1373 K 下的互扩散系数。结果表明，在 CoCrFeNi 高熵合金中添加 Al、Cu 和 Mn 能促进 Co、Cr 和 Fe 原子的扩散。通过对比示踪扩散系数表明，当热力学温度为横坐标时，$Al_{0.2}$CoCrFeNi、CoCr$Cu_{0.2}$FeNi 和 CoCrFe$Mn_{0.2}$Ni 高熵合金的示踪扩散不存在缓慢扩散现象。此外，扩散熵和激活能的线性关系揭示了只要原子的晶体结构不变，组元数量不会影响原子的扩散过程。

关键词：Co−Cr−Fe−Ni；高熵合金；扩散；互扩散系数；扩散偶

(Edited by Bing YANG)